Discover Oncology

Analysis

Arginine methylation modulates tumor fate and prognosis in clear cell renal cell carcinoma

Jiahao Wang[1,2] · Dan Bao[3] · Xiaochao Chen[4] · Zijie Yu[5] · Weiyu Kong[5] · Chen Xu[6] · Songtao Li[1] · Yulin Yue[1]

Received: 16 March 2025 / Accepted: 25 April 2025
Published online: 13 May 2025

Abstract

Background Arginine methylation, a key post-translational modification, plays a pivotal role in regulating various cellular processes and has been implicated in cancer progression. However, the potential of arginine methylation-related genes as prognostic markers in clear cell renal cell carcinoma (ccRCC) remains underexplored.

Methods We utilized public transcriptomic datasets from TCGA, E-MTAB-1980 and ICGC, for model construction and validation. Single-cell RNA sequencing datasets were employed to evaluate gene expression patterns at the cellular level. Consensus clustering, KM survival analysis, and GSVA were applied to identify molecular subtypes and related pathways. Univariate and multivariate Cox regression analyses were applied to develop an arginine methylation-related signature (AMS). Immune profiling, mutation landscape, and drug sensitivity prediction were also employed to explore the model's association with clinical features, immune infiltration, mutation burden, and therapeutic responses.

Results The AMS demonstrated robust prognostic performance, with consistent validation across external cohorts. High-risk patients exhibited significantly worse survival, elevated TMB, and an immunosuppressive tumor microenvironment characterized by increased infiltration of regulatory immune cells. Single-cell RNA sequencing revealed key prognostic genes expressed predominantly in cancer and immune cells, supporting their role in tumor progression and immune interactions.

Conclusion The arginine methylation-based prognostic model provides a reliable framework for survival risk stratification in ccRCC and holds promise for guiding personalized therapeutic strategies. Future research should emphasize clinical validation of this model and explore its potential role in optimizing immunotherapy and targeted treatment strategies for ccRCC.

Keywords Arginine methylation · Clear cell renal cell carcinoma (ccRCC) · Prognostic model · Tumor microenvironment (TME) · Immune infiltration

Jiahao Wang, Dan Bao and Xiaochao Chen have contributed equally to this work.

✉ Chen Xu, chenadoc@126.com; ✉ Songtao Li, songtaoli@njmu.edu.cn; ✉ Yulin Yue, yuelillin@163.com | [1]Department of Clinical Laboratory, Children's Hospital of Nanjing Medical University, Nanjing 210008, China. [2]First Clinical Medical College of Nanjing Medical University, Nanjing 210029, China. [3]Institute of Dermatology & Hospital for Skin Diseases, Chinese Academy of Medical Sciences & Peking Union Medical College, Nanjing 210042, Jiangsu Province, China. [4]Department of Urology, Changhai Hospital, Naval Medical University, Shanghai 200001, China. [5]Department of Urology, The First Affiliated Hospital of Nanjing Medical University, Nanjing 210029, China. [6]Department of Urology, Suzhou Ninth Hospital Affiliated to Soochow University, Suzhou 215200, China.

1 Introduction

Clear cell renal cell carcinoma (ccRCC) is the predominant subtype of kidney cancer, accounting for approximately 70–80% of all renal malignancies [1, 2]. The global incidence of ccRCC has been steadily increasing, and although the 5-year survival rate for patients diagnosed at an early stage is relatively high, prognosis remains poor for those with advanced or metastatic disease [3, 4]. Despite significant advances in treatment options, such as targeted therapy and immunotherapy, challenges such as drug resistance and the need for personalized treatment strategies remain [5, 6]. Therefore, accurate prognostic assessment and the development of tailored therapeutic approaches for ccRCC patients are pressing issues that need to be addressed. Currently, numerous clinical prognostic models have been proposed to predict survival outcomes and recurrence risks in ccRCC patients. However, these models predominantly rely on pathological and clinical features. These models exhibit certain limitations, especially in predicting outcomes for early-stage patients or complex clinical situations where the accuracy of predictions can be compromised. This has prompted increasing interest in identifying molecular biomarkers, particularly those related to post-translational modifications, as a promising direction for improving prognostic accuracy.

Arginine methylation, a crucial post-translational modification, plays a key role in regulating diverse cellular functions, including gene transcription, protein activity, and intracellular signaling [7, 8]. By modifying specific target proteins, it contributes to essential physiological processes such as DNA repair, chromatin remodeling, and protein–protein interactions [9, 10]. Emerging evidence has linked arginine methylation to the initiation and progression of various cancers [11, 12]. In recent years, increasing attention has been directed toward understanding its role in tumor biology, highlighting its potential as a therapeutic target and prognostic biomarker in oncology [13]. Given the potential of arginine methylation to serve as a novel molecular marker, this study aims to explore its characteristics in ccRCC and to develop a prognostic model based on arginine methylation signatures.

In this study, we aimed to investigate the prognostic significance of arginine methylation-related genes in ccRCC. We constructed a novel prognostic model using univariate Cox and LASSO regression analyses, and validated its predictive accuracy across independent external cohorts. Furthermore, we systematically explored the model's associations with immune infiltration, clinical features, mutational landscape, and response to immunotherapy. Single-cell RNA sequencing data were additionally analyzed to assess the expression patterns of model-included genes at the single-cell level, providing insights into their cell-type-specific roles within the tumor microenvironment. This integrative approach offers a foundation for identifying novel biomarkers and developing personalized treatment strategies in ccRCC.

2 Methods

2.1 Data acquisition and preprocessing

We used public transcriptomic datasets from The Cancer Genome Atlas (TCGA) and other external cohorts for our study. The external validation datasets included E-MTAB-1980 and ICGC, which provided additional ccRCC samples for model evaluation. Single-cell RNA sequencing (scRNA-seq) datasets from GSE131685 [14], GSE152938 [15] and GSE171306 [16] were retrieved from Gene Expression Omnibus (GEO) dataset.

2.2 Consensus clustering and pathway analysis

To identify potential subgroups among ccRCC patients, we applied consensus clustering using arginine methylation-related gene expression profiles. Patient classification was performed with the ConsensusClusterPlus R package, followed by Kaplan–Meier (KM) survival analysis to determine the prognostic relevance of the resulting clusters. To further explore their biological characteristics, we conducted Gene Ontology (GO) enrichment and Kyoto Encyclopedia of Genes and Genomes (KEGG) pathway analyses, highlighting key cellular functions and molecular mechanisms. The initial set of arginine methylation-related genes was curated based on a comprehensive literature review [8].

2.3 Construction and validation of prognostic model

To construct a prognostic model, we first applied univariate Cox regression to identify arginine methylation-related genes significantly associated with overall survival ($P < 0.05$). Significant genes were then used to build a multivariate Cox model, and the arginine methylation-related signature (AMS) was derived by calculating a weighted sum of gene

expression levels based on regression coefficients. Patients were stratified into high- and low-risk groups using the median AMS score. Kaplan–Meier survival analysis and time-dependent ROC curves were used to evaluate the model's predictive performance. To assess whether AMS serves as an independent prognostic factor, multivariate Cox regression was performed including age, sex, tumor stage, and grade as covariates. The model was further validated in two external datasets (E-MTAB-1980 and ICGC), where AMS consistently showed strong prognostic value and generalizability.

2.4 Immune profiling and tumor microenvironment analysis

Immune cell infiltration was estimated using the ssGSEA algorithm. We also performed immune subtype classification and evaluated the relationship between immune cell populations and the AMS. Immune subtypes (C1–C6) were assigned to ccRCC samples according to the TCGA pan-cancer classification described by Thorsson et al. [17]. The relationship between immune function and the AMS was analyzed using functional immune scores, including antigen presentation, immune checkpoint activity, and immune-related signaling pathways.

2.5 Mutation landscape and immunotherapy analysis

We examined the mutation landscape in high- and low-risk groups by analyzing the mutation frequency. Tumor mutation burden (TMB) was calculated for its association with the AMS was analyzed. Survival analysis was performed in the IMvigor210 cohort to evaluate the relationship between AMS and patient response to immune checkpoint blockade therapy.

2.6 Drug sensitivity analysis

To evaluate the association between AMS scores and drug response in ccRCC, we utilized the Genomics of Drug Sensitivity in Cancer (GDSC) database [18]. The half-maximal inhibitory concentration (IC50) values of various drugs were analyzed and compared between high and low-risk groups to identify potential therapeutic agents with differential efficacy.

2.7 Single-cell RNA sequencing analysis

Single-cell RNA sequencing (scRNA-seq) data from GSE131685, GSE152938, and GSE171306 were processed using the Seurat R package (v4.0) to analyze the expression patterns of prognostic genes in ccRCC. Cells with fewer than 200 detected genes or more than 10% mitochondrial gene content were filtered out. Gene expression was normalized using the LogNormalize method, followed by identification of highly variable genes and data scaling. Principal component analysis (PCA) was performed for dimensionality reduction, and clusters were identified using the FindClusters function (resolution = 0.5). UMAP was used for visualization. Cell types were annotated based on canonical markers, and the distribution of cancer, immune, and stromal cells was compared between ccRCC and normal tissues. The model genes (CARM1, PRMT1, PRMT5, PRMT9) were primarily expressed in cancer and immune cells, as shown by violin and UMAP feature plots, supporting their potential roles in tumor progression and immune regulation.

3 Results

3.1 Consensus clustering and pathway analysis

Based on the expression profile of IREs, patients were stratified into three molecular subtypes: Clusters A, B, and C (Fig. 1A). Kaplan–Meier survival analysis revealed significant differences in survival outcomes between the clusters, indicating their potential prognostic value (Fig. 1B). The heatmap of clinical features further highlighted the correlation between clinical characteristics and the identified clusters (Fig. 1C). The Venn diagram illustrated the overlap of differentially expressed genes between three clusters, emphasizing 916 common genes, and offering insight into shared molecular signatures across the clusters (Fig. 1D). GO analysis identified key biological processes and molecular functions, such as mRNA splicing and histone modification (Fig. 1E). KEGG analysis revealed significantly enriched pathways, including MAPK signaling, ribosome biogenesis, and cancer-related pathways, highlighting the molecular pathways involved in the disease (Fig. 1F). Finally, GSVA analysis displayed differential expression of these pathways across clusters, suggesting

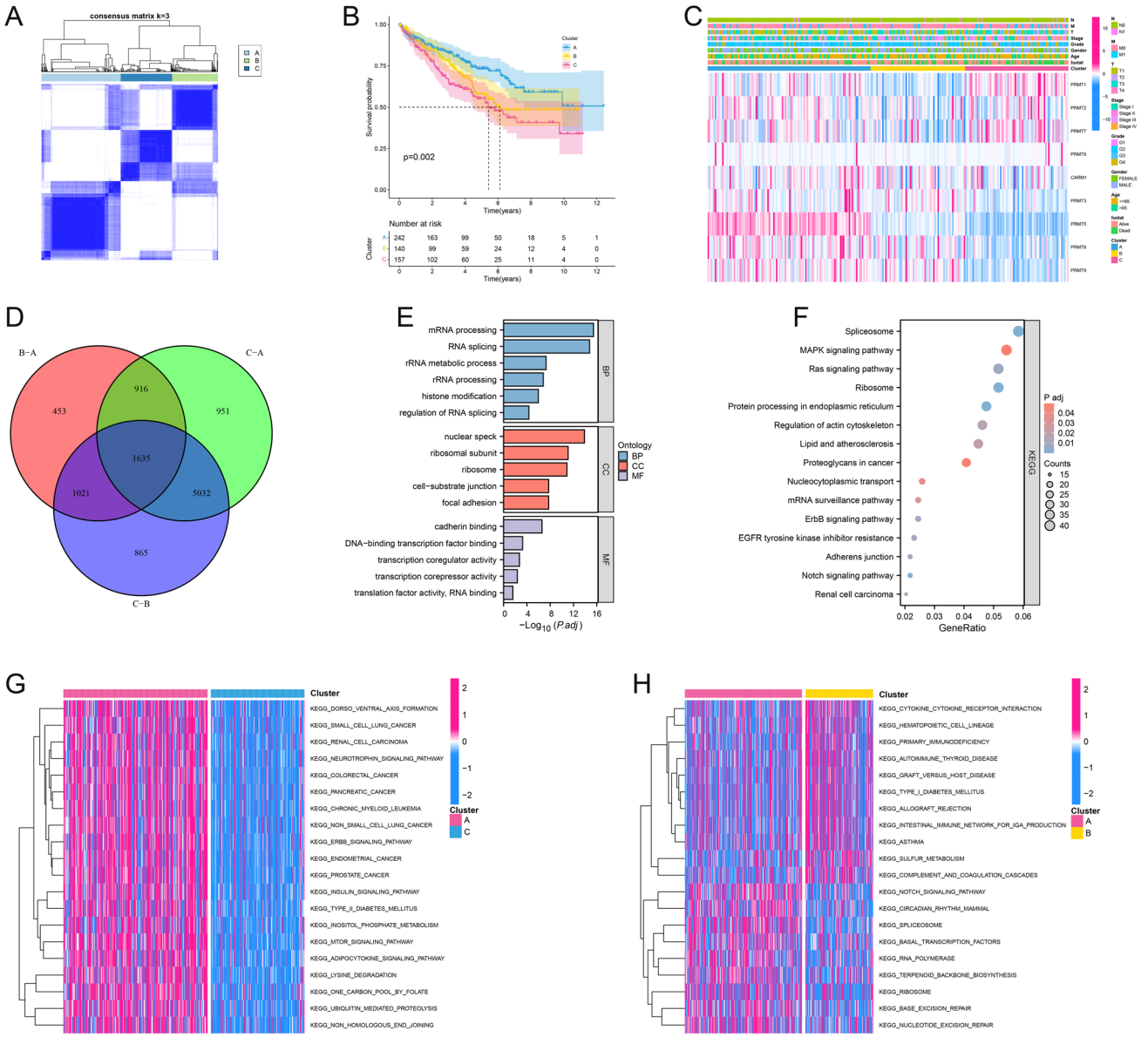

Fig. 1 Consensus clustering and functional analysis. **A** Consensus clustering matrix for three clusters based on arginine methylation genes. **B** KM survival curves showing survival differences between clusters (log-rank test, $p < 0.001$). **C** Heatmap of clinical and gene expression across clusters. **D** Venn diagram of differentially expressed genes among clusters. **E**, **F** GO and KEGG enrichment analysis of biological processes in clusters. **G**, **H** GSVA analysis highlighting enriched pathways

distinct molecular profiles in cancer (Fig. 1G, H). Together, these results provide a detailed understanding of the molecular mechanisms and clinical relevance of ccRCC.

3.2 Construction and validation of arginine methylation-related signature

Univariate Cox regression analysis identified several genes significantly associated with prognosis ($p < 0.001$), where PRMT9 and PRMT5 were protective factors, whereas CARM1 and PRMT7 were linked to poor survival (Fig. 2A). Multivariate Cox regression was adopted to construct the arginine methylation signature (AMS) (Fig. 2B). The AMS distribution and survival status plots demonstrate high-risk patients exhibiting worse survival outcomes (Fig. 2C, D). The predictive accuracy of the model was evaluated using ROC curves, with AUC values of 0.710, 0.647, and 0.663 at 1, 2, and 3 years, respectively (Fig. 2E). Additionally, univariate and multivariate Cox regression analyses incorporating clinical features confirmed that AMS remained an independent prognostic factor (Fig. 2F and G). External validation using E-MTAB-1980

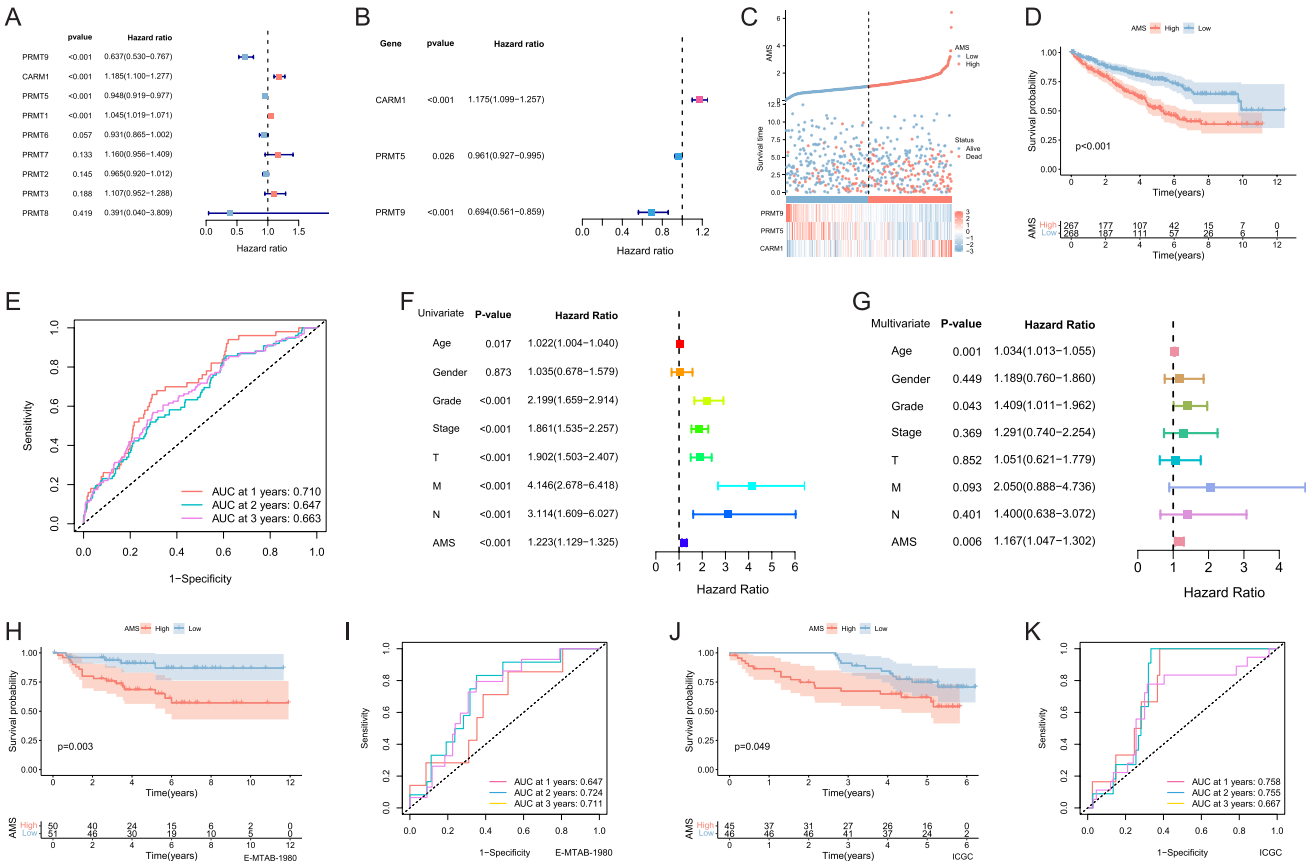

Fig. 2 Prognostic model construction and validation. **A**, **B** Univariate and multivariate Cox regression analyses of key arginine methylation-related genes. **C**, **D** Distribution and survival analysis of patients classified into high- and low-AMS groups. **E** ROC curve evaluating the predictive accuracy of the AMS. **F**, **G** Univariate and multivariate Cox regression analysis of clinical factors and AMS. **H**–**K** KM survival curve and ROC for AMS in the E-MTAB-1980 and ICGC cohorts (log-rank test, $p < 0.001$)

and ICGC datasets demonstrated that high-risk patients showed significantly worse survival (Fig. 2H and J). ROC analysis in these validation cohorts further confirmed the model's robustness, with AUC values exceeding 0.7 in most cases (Fig. 2I and K).

3.3 Immune profiling of arginine methylation-related signature

The heatmap illustrated distinct patterns of immune cell infiltration between high- and low-AMS groups, indicating divergent immune landscapes associated with risk stratification (Fig. 3A). The correlation analysis further explored the associations between immune cell infiltration and AMS, showing that specific immune cell populations exhibit significant positive or negative correlations with the prognostic risk (Fig. 3B). The boxplots demonstrated the distribution of AMS across different immune subtypes, with immune subtype C6 exhibiting significantly higher AMS compared to other subtypes. Notably, C6 has been associated with an immunosuppressive phenotype and poor prognosis, suggesting that patients with this immune subtype may experience worse survival outcomes (Fig. 3C). The violin plots compared the abundance of key immune cell populations, including regulatory T cells, myeloid-derived suppressor cells (MDSCs), and macrophages, between high- and low-risk groups, showing a higher infiltration of immunosuppressive cells in the high-risk group (Fig. 3D). Boxplots of immune function scores showed significant differences in pathways related to antigen presentation, immune checkpoint activity, and cytokine signaling between risk groups (Fig. 3E). The ESTIMATE analysis evaluated the tumor microenvironment scores, demonstrating that high-risk group exhibited significantly higher immune and stromal scores, suggesting a more immunosuppressive tumor microenvironment (Fig. 3F). Moreover, AMS was positively associated with key immune responses, including Treg cells, macrophages and MDSCs (Fig. 3G). Collectively, these findings highlighted the

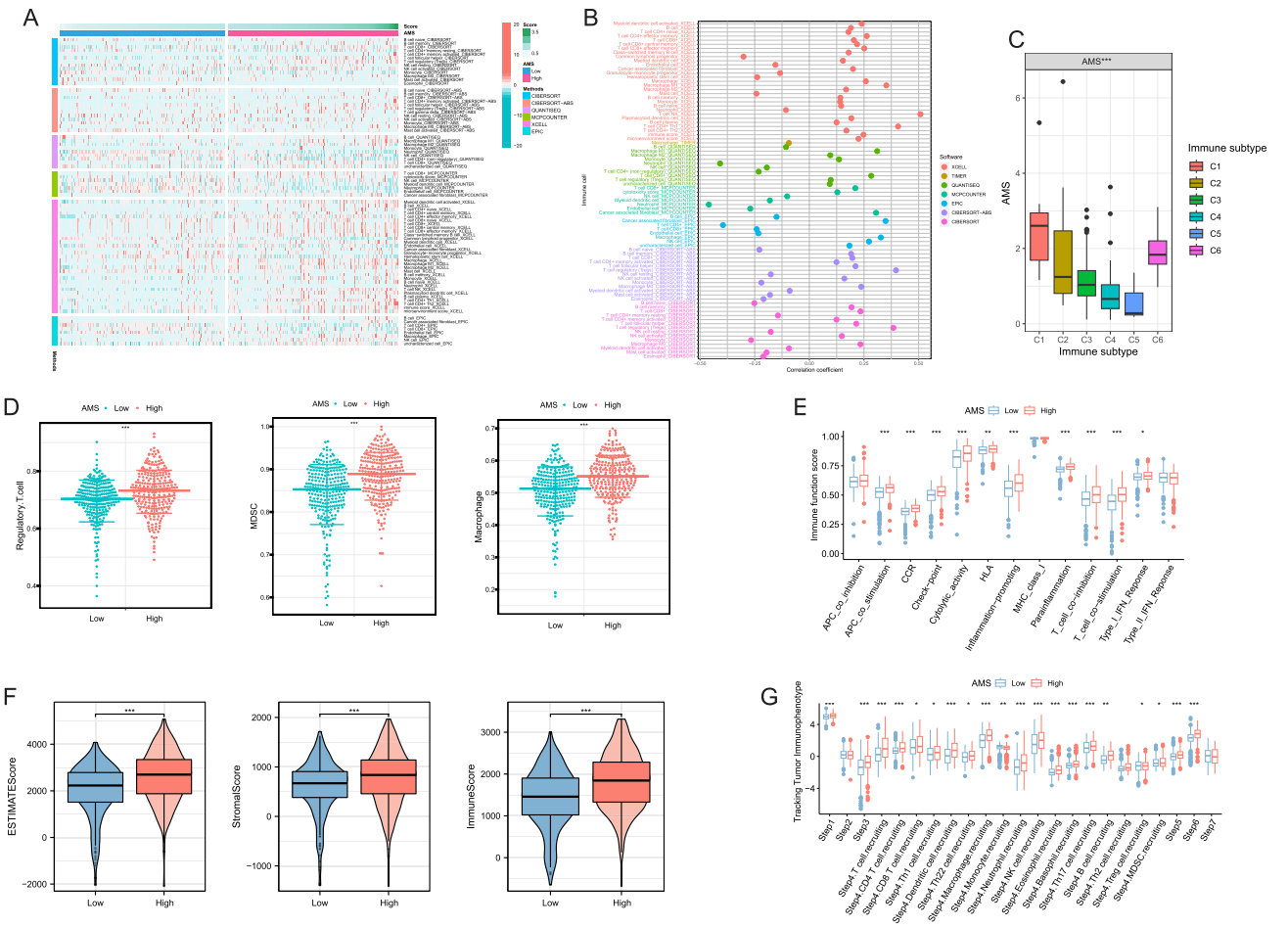

Fig. 3 Immune landscape analysis based on the arginine methylation-related signature. **A**, **B** Expression and correlation analysis between AMS and immune cell infiltration levels. **C** Boxplot comparing AMS scores across different immune subtypes (Kruskal–Wallis test, $p < 0.001$). **D** Differential expression of immunosuppressive cells between AMS groups (Wilcoxon test, *$p < 0.01$). **E** Immune function scores in high- and low-AMS groups (Wilcoxon test, $p < 0.05$ to $p < 0.001$). **F** Comparison of TME scores between high- and low-AMS groups (Wilcoxon test, $p < 0.001$). **G** Tracking Tumor Immunophenotype analysis of immune responses in high- and low-AMS groups

distinct immune landscape between high- and low-AMS patients, suggesting that the prognostic model was closely associated with the tumor immune microenvironment and could serve as a potential biomarker for predicting immunotherapy outcomes in ccRCC.

3.4 Clinical correlation and prognostic value of arginine methylation-related signature

Analysis of clinical features revealed a strong association between AMS and disease severity in ccRCC. Specifically, risk scores were significantly higher in patients with advanced tumor grade (G3–G4), later clinical stage (Stage III–IV), higher T classification (T3–T4), presence of distant metastasis (M1), and lymph node involvement (N1), as demonstrated by stratified boxplots (Fig. 4A). Chi-square analysis further supported these findings by showing that high-risk patients were disproportionately distributed among clinically aggressive subgroups (Fig. 4B). Moreover, Kaplan–Meier survival analyses across stratified clinical parameters confirmed that high-risk patients consistently exhibited poorer overall survival, even within early-stage (Stage I–II), low-grade (G1–G2), non-metastatic (M0), and node-negative (N0) populations (Fig. 4C). These results underscore the ability of AMS to reflect tumor aggressiveness and its robustness as an independent prognostic indicator across various clinical contexts in ccRCC.

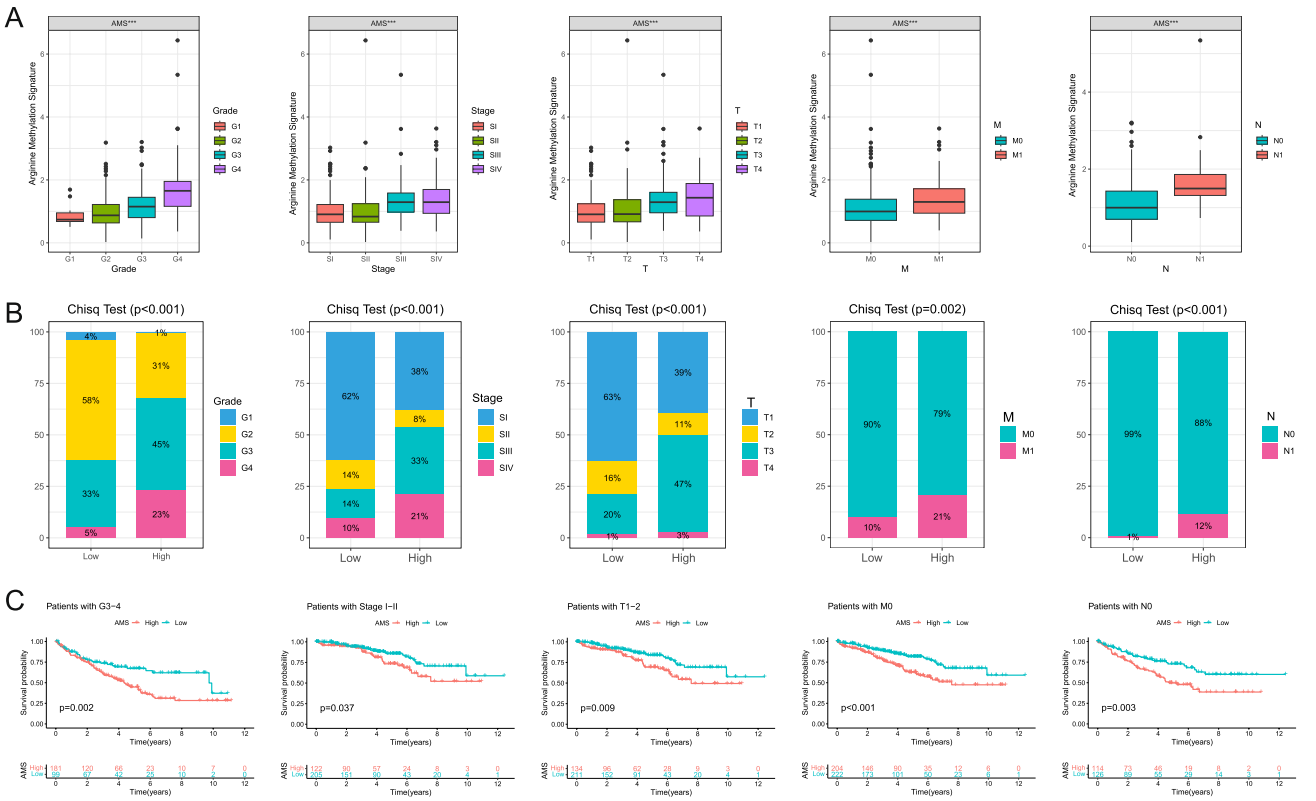

Fig. 4 Clinical correlation and prognostic value of the arginine methylation-related signature. **A** Distribution of AMS across different clinical parameters (Wilcoxon test, *p < 0.01 to p < 0.001). **B** Proportion of patients in high and low AMS groups for each clinical parameter (Chi-square test, p < 0.05). **C** KM survival curves showing significant differences in survival outcomes between AMS groups within specific subgroups (log-rank test, p < 0.05 to p < 0.001)

3.5 Mutation landscape and immunotherapy characteristics of arginine methylation-related signature

Comprehensive mutational analysis revealed that the high-risk group exhibited a markedly higher mutation frequency compared to the low-risk group (Fig. 5A–B). A strong positive correlation was observed between AMS and tumor mutation burden (TMB), which was further supported by significantly elevated TMB levels in the high-risk group, as shown in scatter and boxplots (Fig. 5C–D). Survival analysis demonstrated that patients with high TMB had worse overall survival, and stratification by both TMB and AMS indicated that individuals with concurrent high TMB and high AMS experienced the poorest prognoses, suggesting a synergistic negative impact on patient outcomes (Fig. 5E–F). Additionally, immune checkpoint molecules—including PDCD1, CTLA4, and TIGIT—were significantly upregulated in the high-risk group, implying an association between AMS and immune escape mechanisms (Fig. 5G). In the IMvigor210 immunotherapy cohort, high-risk patients exhibited significantly worse survival, and ROC analysis confirmed the predictive value of the AMS in the context of immune checkpoint blockade (Fig. 5H–I). Moreover, AMS scores were significantly higher in non-responders compared to responders, and Chi-square analysis showed distinct differences in immunotherapy response rates between high- and low-risk groups (Fig. 5J–K). Collectively, these findings indicate that AMS is closely linked to mutational burden, immune checkpoint activation, and clinical response to immunotherapy, underscoring its potential as a predictive biomarker for guiding immunotherapeutic strategies in ccRCC.

3.6 Drug sensitivity analysis of arginine methylation-related signature

Figure 6 illustrated the correlation between the AMS and drug sensitivity in ccRCC, demonstrating significant differences in drug response between high- and low-risk groups. The boxplots compared the estimated IC50 values for multiple therapeutic agents, revealing that high-risk patients exhibited significantly lower sensitivity to Temsirolimus (A), Sunitinib (B), and Sorafenib (C), suggesting potential resistance to these commonly used targeted therapies. Conversely, the

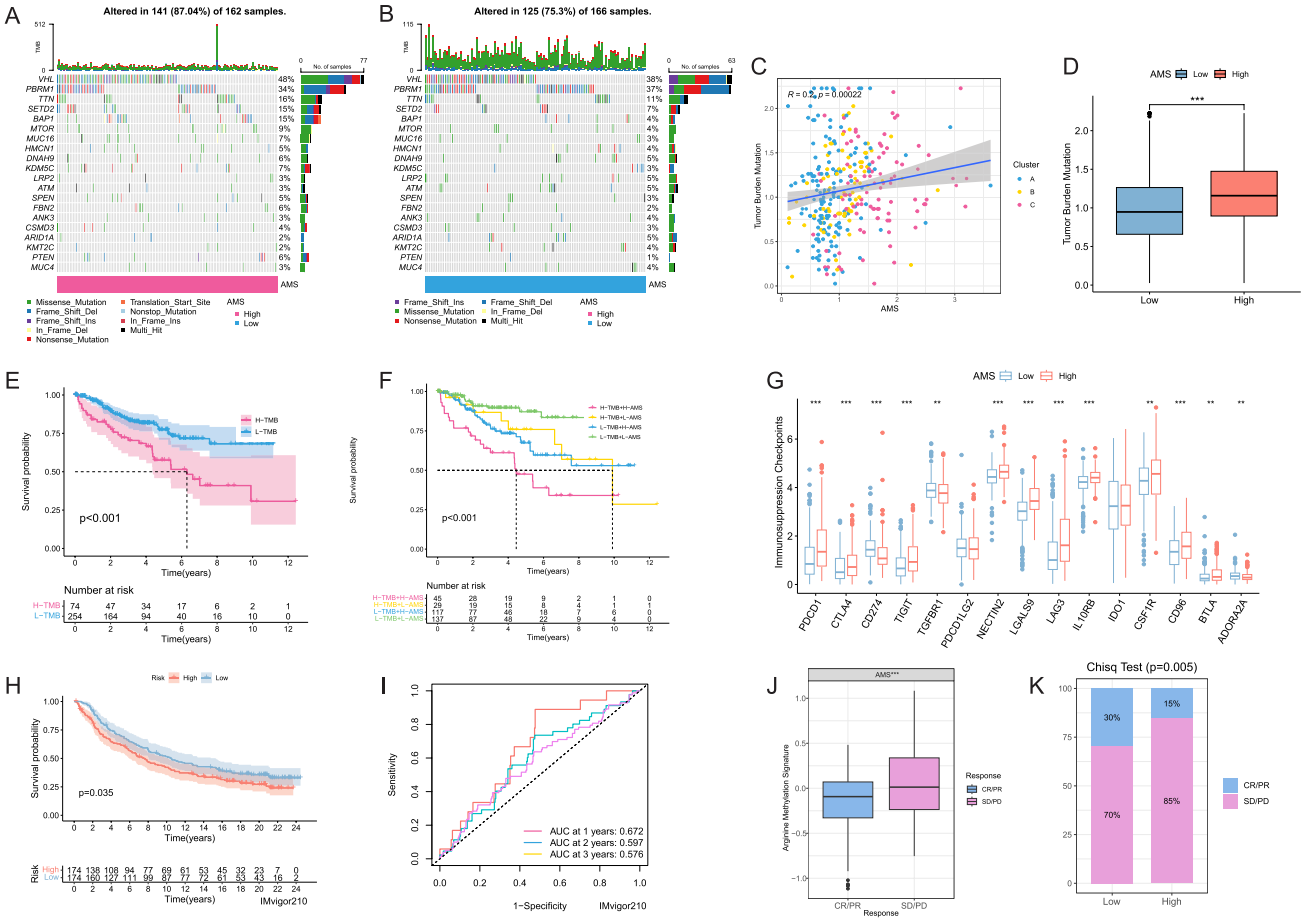

Fig. 5 Mutation landscape and immune checkpoint analysis based on the arginine methylation-related signature (AMS) in ccRCC. **A**, **B** Mutation landscape of frequently altered genes in the high-AMS (**A**) and low-AMS (**B**) groups. **C** Correlation of TMB and AMS (Spearman's correlation, $p < 0.001$). **D** Comparison of TMB between high- and low-AMS groups (Wilcoxon test, $p < 0.001$). **E** KM survival analysis of ccRCC patients stratified by TMB (log-rank test, *$p < 0.01$). **F** Combined survival analysis of TMB and AMS (log-rank test, $p < 0.001$). **G** Comparison of immune checkpoints between high- and low-AMS groups (Wilcoxon test, $p < 0.05$ to $p < 0.001$). **H–I** KM survival and ROC analysis of AMS groups in the IMvigor 210 immunotherapy cohort (log-rank test, *$p < 0.01$). **J** Comparison of AMS between patients with different immunotherapy responses (Wilcoxon test, $p < 0.05$). **K** Distribution of AMS between CR/PR and SD/PD response groups (Chi-square test, $p < 0.05$)

high-risk group showed increased sensitivity to Pazopanib (D), Bosutinib (E), Lenalidomide (F), Vorinostat (G), Nilotinib (H), and Metformin (I), indicating that these agents may be more effective for patients classified as high-risk. These findings suggested that the prognostic model can help predict differential drug responses, providing insights into potential personalized treatment strategies for ccRCC patients.

3.7 Single-cell analysis of prognostic model genes in ccRCC

Figure 7 presented the scRNA-seq analysis of the genes incorporated in the prognostic model, highlighting their expression across different cell types in ccRCC and normal tissues. The UMAP plots displayed the distribution of ccRCC and normal samples, showing distinct cellular compositions between tumor and normal tissues (Fig. 7A). The cell type annotation map identified major cell populations (Fig. 7B). The bar plots further illustrated the proportion and number of different cell types between ccRCC and normal samples, revealing an increased presence of cancer and immune-related cells in ccRCC (Fig. 7C, D). The violin plots depicted the expression levels of key prognostic genes (CARM1, PRMT1,

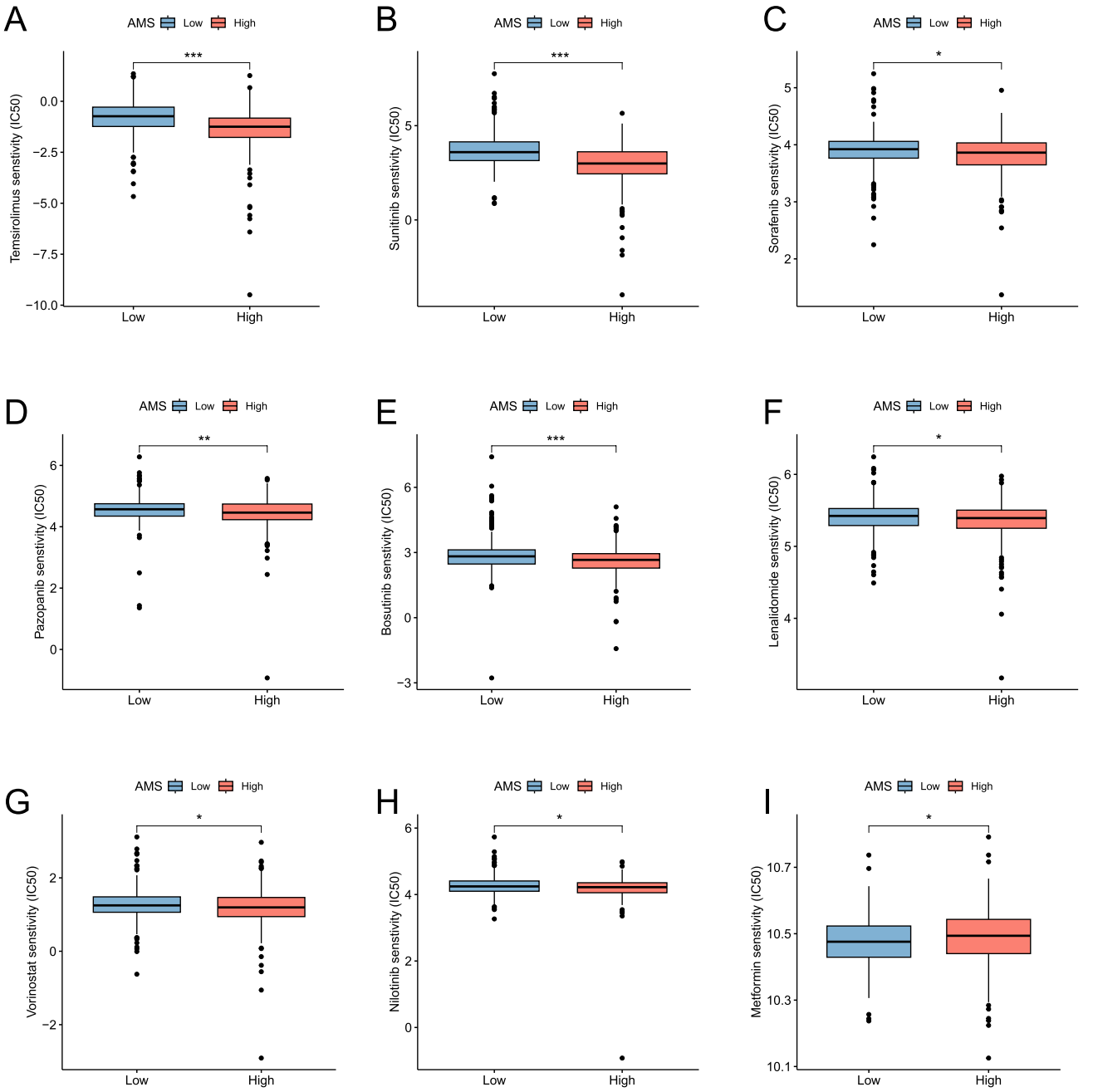

Fig. 6 Drug sensitivity analysis based on the arginine methylation-related signature. **A**–**I** Boxplots showing the sensitivity (IC50) of various drugs in AMS groups: (**A**) Temsirolimus, (**B**) Sunitinib, (**C**) Sorafenib, (**D**) Pazopanib, (**E**) Bosutinib, (**F**) Lenalidomide, (**G**) Vorinostat, (**H**) Nilotinib, (**I**) Metformin (Wilcoxon test, $p < 0.05$ to $p < 0.001$)

PRMT5, PRMT9) across various cell types, showing their predominant expression in cancer cells and immune components (Fig. 7E–H). Finally, the UMAP feature plots visualized the spatial expression patterns of these genes in ccRCC and normal tissues, demonstrating their enrichment in tumor-associated regions (Fig. 7I–L). These findings provided valuable insights into the cellular localization and potential functional roles of prognostic model genes in ccRCC, further supporting their relevance in tumor progression and immune interactions.

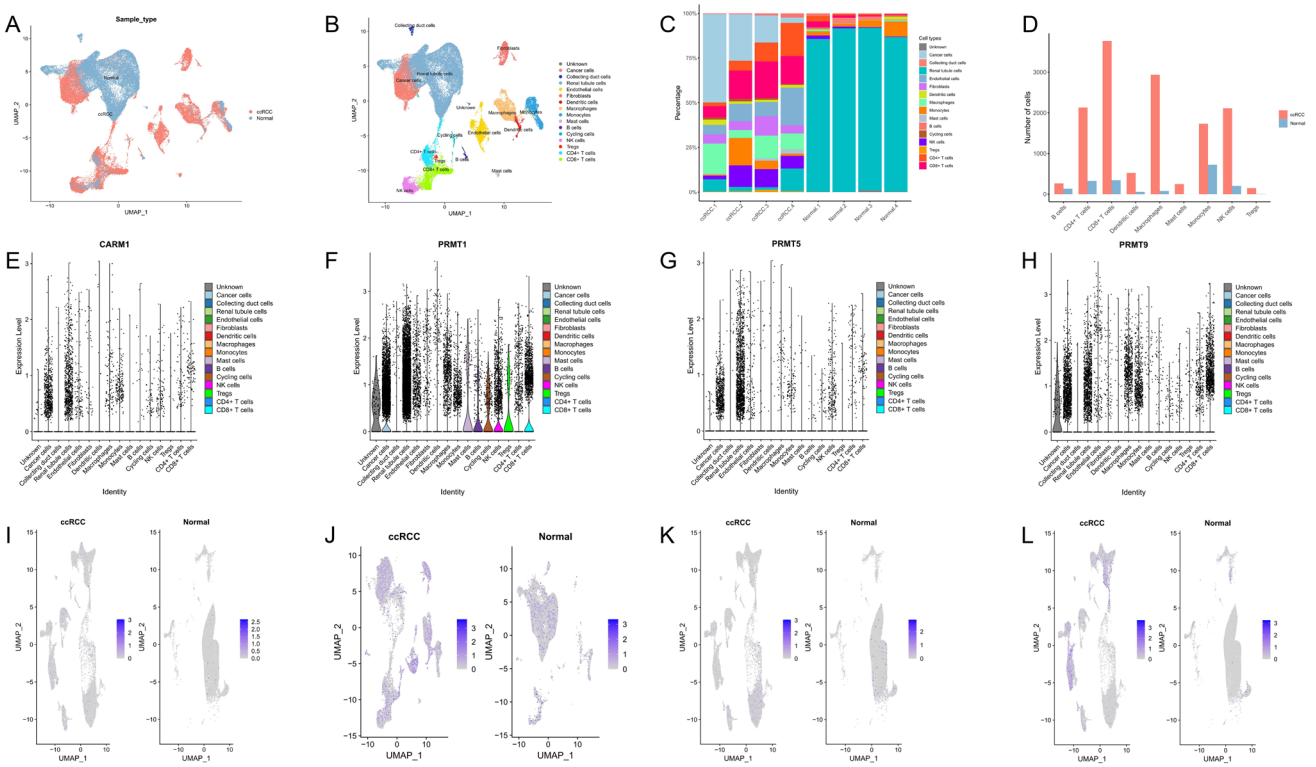

Fig. 7 Single-cell RNA sequencing analysis of arginine methylation-related genes. **A** Distribution of cancer and normal samples across cell types in ccRCC. **B** UMAP plot colored by the identity of different cell types. (**C**) Proportion of different cells in each sample. (**D**) Bar plot illustrating the proportion of various cell types across cancer and normal tissues. (**E**–**H**) Expression levels of CARM1, PRMT1, PRMT5, PRMT9 across different cell types. (**I**-**L**) UMAP plots illustrating the expression of CARM1, PRMT1, PRMT5, and PRMT9 across ccRCC and normal tissue samples

4 Discussion

The prognostic model developed in this study held significant potential in clinical applications, particularly for personalized treatment strategies and prognostic monitoring in ccRCC. Arginine methylation, as a key post-translational modification, plays a crucial role in regulating gene expression, RNA processing, and protein interactions, and its dysregulation has been increasingly implicated in tumorigenesis [9, 19]. By integrating multiple arginine methylation-related genes into a risk model, we established a novel method for predicting patient outcomes and stratifying patients based on molecular characteristics rather than solely on clinical parameters.

In clinical practice, this model could serve as a valuable tool for individualized risk assessment. Patients classified as high-risk may require more intensive follow-up and could benefit from alternative therapeutic strategies, while low-risk patients may avoid unnecessary aggressive treatments, thereby reducing potential side effects. Furthermore, our analysis of drug sensitivity suggests that high-risk patients exhibit resistance to standard tyrosine kinase inhibitors (TKIs) but may respond better to alternative agents, such as metabolic and epigenetic modulators, which could guide personalized therapeutic decisions. Additionally, since our model is closely associated with immune infiltration patterns, it may help predict response to immunotherapy, aiding in the selection of patients who are more likely to benefit from immune checkpoint inhibitors. Several prognostic models for ccRCC have been proposed based on gene expression, DNA methylation, and immune signatures. Compared to traditional models that primarily rely on clinical features (e.g., TNM staging and Fuhrman grading), molecular-based models provide a deeper understanding of tumor biology and allow for more refined risk stratification. Recent studies have explored prognostic models based on gene expression profiling, identifying tumor-associated pathways and immune signatures as key determinants of patient outcomes [20, 21]. However, these models often fail to capture post-translational regulatory mechanisms, which are crucial for understanding tumor progression and therapeutic resistance. While DNA methylation is a critical regulatory mechanism, it primarily affects transcriptional activity and does not fully account for post-translational modifications,

such as arginine methylation, that influence protein function and signaling pathways [22, 23]. Compared to these models, our study highlighted the unique contribution of arginine methylation in ccRCC prognosis, suggesting that protein-level regulatory modifications may play an equally, if not more, significant role in disease progression and therapeutic response.

Arginine methylation is a critical post-translational modification involved in regulating gene expression, RNA processing, and protein–protein interactions [24, 25]. Increasing evidence suggests that dysregulation of arginine methylation contributes to tumor progression, particularly by influencing oncogenic signaling and immune modulation [26, 27]. Our study identified key arginine methylation-related genes that were significantly related to ccRCC prognosis, indicating their potential roles in tumor aggressiveness and therapeutic resistance. The strong association between AMS and TME further suggested that arginine methylation may have a significant effect in shaping TME, potentially affecting immune evasion mechanisms and treatment responses. Our immune infiltration research showed that high-AMS ccRCC patients exhibited an immunosuppressive TME, characterized by increased infiltration of regulatory T cells, MDSCs, and macrophages. Notably, we found a strong correlation between high-AMS and immune subtype C6, which has been linked to poor prognosis and an exhausted immune phenotype. This suggested that high-AMS groups may be more resistant to immune checkpoint blockade (ICB) therapy due to an immune-excluded or immune-suppressive TME. While immune checkpoint molecules such as PDCD1, CTLA4, and TIGIT were obviously upregulated in high-AMS group, our analysis indicated significant difference in actual immunotherapy response rates in AMS groups. This outcome suggested that not only immune checkpoint expression was elevated, but also other factors—such as T-cell exhaustion, myeloid-driven immune suppression, and stromal-mediated immune exclusion—may contribute to immune escape in high-risk ccRCC patients. It should also be noted that the IMvigor210 cohort used for immunotherapy validation originates from patients with advanced urothelial carcinoma. Although it has been widely adopted in immune signature studies across tumor types, its extrapolation to ccRCC is indirect and should be interpreted with caution. Future studies involving ccRCC-specific immunotherapy cohorts would further enhance the robustness of our findings. While our single-cell analysis revealed the expression patterns of AMS genes across various cell types, it remains primarily descriptive. Future studies incorporating pathway activity inference and cell–cell communication analysis (e.g., using CellChat or NicheNet) are needed to elucidate how AMS genes functionally shape the tumor microenvironment and intercellular dynamics in ccRCC.

Despite the strengths of our study, several limitations should be acknowledged. First, our prognostic model was constructed and validated using retrospective transcriptomic datasets, and prospective validation in clinical cohorts is needed to confirm its real-world applicability. Second, while our single-cell analysis provided insights into the cellular localization of model genes, functional validation through in vitro and in vivo experiments is required to elucidate their precise roles in ccRCC progression and therapy resistance. Third, the relationship between arginine methylation and immune evasion remains largely unexplored, and further mechanistic studies are needed to determine how these modifications influence TME remodeling and immune checkpoint regulation. Additionally, given the observed drug resistance patterns, future research should focus on testing combination therapies that target both arginine methylation pathways and immune escape mechanisms in ccRCC.

5 Conclusion

Our study demonstrated that arginine methylation-related genes play a crucial role in ccRCC progression and immune regulation. The prognostic model we developed provided a valuable tool for risk stratification and treatment decision-making, highlighting the need for personalized therapeutic strategies. Future research should focus on experimental validation and clinical translation of these findings to improve treatment outcomes in ccRCC patients.

Acknowledgements Not applicable.

Author contributions Jiahao Wang, Dan Bao and Xiaochao Chen contributed equally to this work and were responsible for data collection, analysis, and manuscript drafting. Zijie Yu and Weiyu Kong participated in data validation, statistical analysis, and visualization. Chen Xu, Songtao Li, and Yulin Yue supervised the study, provided conceptual guidance, and revised the manuscript critically for important intellectual content. All authors read and approved the final manuscript.

Funding This work was supported by the project of Nanjing health science and technology development special fund (ZKX23048) to Yulin Yue, the Youth Project of "Gusu healthy" (GSWS2022110) to Chen Xu, the Youth Project of Suzhou City (QNXM2024084) to Chen Xu, and the Project of Jiangsu Province (Z2024061) to Chen Xu.

Availability of data and materials The datasets generated and/or analysed during the current study are available in the TCGA and GEO datasets repository.

Declarations

Ethics approval and consent to participate Not applicable.

Consent for publication The authors confirm that all necessary consent for publication has been obtained from relevant parties.

Competing interests The authors declare no competing interests.

References

1. Jonasch E, Walker CL, Rathmell WK. Clear cell renal cell carcinoma ontogeny and mechanisms of lethality. Nat Rev Nephrol. 2021;17(4):245–61.
2. Bray F, et al. Global cancer statistics 2018: GLOBOCAN estimates of incidence and mortality worldwide for 36 cancers in 185 countries. CA Cancer J Clin. 2018;68(6):394–424.
3. Li QK, et al. Challenges and opportunities in the proteomic characterization of clear cell renal cell carcinoma (ccRCC): a critical step towards the personalized care of renal cancers. Semin Cancer Biol. 2019;55:8–15.
4. Wettersten HI, et al. Metabolic reprogramming in clear cell renal cell carcinoma. Nat Rev Nephrol. 2017;13(7):410–9.
5. Young M, et al. Renal cell carcinoma. Lancet. 2024;404(10451):476–91.
6. Chen S, et al. Deep learning-based multi-model prediction for disease-free survival status of patients with clear cell renal cell carcinoma after surgery: a multicenter cohort study. Int J Surg. 2024;110(5):2970–7.
7. Zhang B, et al. Arginine methylation and respiratory disease. Transl Res. 2024;272:140–50.
8. Guccione E, Richard S. The regulation, functions and clinical relevance of arginine methylation. Nat Rev Mol Cell Biol. 2019;20(10):642–57.
9. Wu Q, et al. Protein arginine methylation: from enigmatic functions to therapeutic targeting. Nat Rev Drug Discov. 2021;20(7):509–30.
10. Fong JY, et al. Therapeutic targeting of RNA splicing catalysis through inhibition of protein arginine methylation. Cancer Cell. 2019;36(2):194-209.e9.
11. Zheng K, et al. Protein arginine methylation in viral infection and antiviral immunity. Int J Biol Sci. 2023;19(16):5292–318.
12. Cheung N, et al. Protein arginine-methyltransferase-dependent oncogenesis. Nat Cell Biol. 2007;9(10):1208–15.
13. Xu J, Richard S. Cellular pathways influenced by protein arginine methylation: Implications for cancer. Mol Cell. 2021;81(21):4357–68.
14. Liao J, et al. Single-cell RNA sequencing of human kidney. Sci Data. 2020;7(1):4.
15. Su C, et al. Single-cell RNA sequencing in multiple pathologic types of renal cell carcinoma revealed novel potential tumor-specific markers. Front Oncol. 2021;11: 719564.
16. Yu Z, et al. Single-cell RNA-seq identification of the cellular molecular characteristics of sporadic bilateral clear cell renal cell carcinoma. Front Oncol. 2021;11: 659251.
17. Thorsson V, et al. The immune landscape of cancer. Immunity. 2018;48(4):812-830.e14.
18. Yang W, et al. Genomics of drug sensitivity in cancer (GDSC): a resource for therapeutic biomarker discovery in cancer cells. Nucl Acid Res. 2013;41:D955-61.
19. Fuhrmann J, Clancy KW, Thompson PR. Chemical biology of protein arginine modifications in epigenetic regulation. Chem Rev. 2015;115(11):5413–61.
20. Wei K, Zhang X, Yang D. Identification and validation of prognostic and tumor microenvironment characteristics of necroptosis index and BIRC3 in clear cell renal cell carcinoma. PeerJ. 2023;11: e16643.
21. Wang W, et al. A novel signature constructed by differential genes of muscle-invasive and non-muscle-invasive bladder cancer for the prediction of prognosis in bladder cancer. Front Immunol. 2023;14:1187286.
22. Di Lorenzo A, Bedford MT. Histone arginine methylation. FEBS Lett. 2011;585(13):2024–31.
23. Bedford MT, Clarke SG. Protein arginine methylation in mammals: who, what, and why. Mol Cell. 2009;33(1):1–13.
24. Blanc RS, Richard S. Arginine methylation: the coming of age. Mol Cell. 2017;65(1):8–24.
25. Chen C, et al. Deciphering arginine methylation: Tudor tells the tale. Nat Rev Mol Cell Biol. 2011;12(10):629–42.
26. Kaushik S, et al. Genetic deletion or small-molecule inhibition of the arginine methyltransferase PRMT5 exhibit anti-tumoral activity in mouse models of MLL-rearranged AML. Leukemia. 2018;32(2):499–509.
27. Yang L, et al. PRMT5 functionally associates with EZH2 to promote colorectal cancer progression through epigenetically repressing CDKN2B expression. Theranostics. 2021;11(8):3742–59.